IEEE Access
Multidisciplinary ⋮ Rapid Review ⋮ Open Access Journal

Received 11 July 2024, accepted 28 July 2024, date of publication 2 August 2024, date of current version 12 August 2024.

Digital Object Identifier 10.1109/ACCESS.2024.3437242

RESEARCH ARTICLE

An Ultrawideband Spiral Antenna With a Stable Phase Center

AMIRHOSSEIN MOUSAVIKHAH[1], VAHID NAYYERI[1], (Senior Member, IEEE), AND MOSTAFA KHANJARIAN[2]

[1]School of Advanced Technologies, Iran University of Science and Technology, Tehran 16846-13114, Iran
[2]School of Electrical Engineering, Iran University of Science and Technology, Tehran 16846-13114, Iran

Corresponding author: Vahid Nayyeri (nayyeri@iust.ac.ir)

ABSTRACT This article introduces an ultrawideband antenna with stable phase center and circular polarization. The proposed antenna is a low-profile cavity-backed spiral antenna measuring 58 × 58 × 50 mm^3, where the cavity is partially filled with an absorber. Throughout the desired frequency range of 2 GHz to 18 GHz, the antenna maintains a return loss better than 10 dB; the phase center offset remains within 10 mm in the direction of radiation and 4 mm in the plane of the spiral arms, the phase center variation is less than 6 degrees; and the axial ratio of less than 3 dB. Fabrication and measurements of the antenna serve to validate its performance.

INDEX TERMS Axial ratio, cavity backed, circular polarization, phase center offset, phase center variation, spiral antenna, ultrawideband antenna.

I. INTRODUCTION

In an ideal scenario, in the far-field region of an antenna, on a spherical surface centered at a point known as the antenna phase center, the phase of radiated signal (or equivalently radiation pattern) remains constant [1]. However, in reality, our observation is different: the phase is not constant and vary with spatial angles [2]. These changes are due to factors such as asymmetry in the physical structure of the antenna, asymmetry in the radiation pattern of the antenna, surface currents on the antenna, and imbalance. Phase changes in the antenna are frequency-dependent, causing the antenna phase center to change with a frequency. In other words, in a wideband antenna, a fixed reference point for the antenna phase center cannot be obtained.

On the other hand, the stability of the phase center is of the importance in various applications such as, navigation [1], [2], [3], communication [4], satellite positioning [5], reflector antenna feeding [6], and direction finding (DF). Phase comparison-based DF algorithms [7], [8] rely on the phase of the received signal by the antenna element with respect to its phase center. Then through the signal processing techniques the accurate position of the signal source is determined. Therefore, precise estimation of the antenna phase center and its stability leads to higher accuracy and reduced error in detecting the location of the signal source. In navigation systems such as GPS, antennas with a stable phase center also provide higher positional accuracy [9]. Furthermore, in the design of reflector antennas, locating the phase center of the feed antenna at the focal point of the reflector is essential; hence, the stability of the phase center across the operating bandwidth (BW) contributes to increased radiation efficiency of the reflector antenna.

In literature, various types of wideband antennas with stable phase centers can be found. These include horn antennas [4], [10], [11], [12], rod antennas [13], [14], Vivaldi antennas [15], [16], [17], Slot antennas [18], helical antennas [19], and spiral antennas [20], [21], [22]. In [11], a ridged horn antenna with a relatively stable phase center and linear polarization was presented in the Ka-band. Another example of a horn antenna with a relatively stable phase center and linear polarization in the frequency band of 8-20 GHz is reported in [4]. However, the use of horn antennas at lower frequencies results in large and heavy structures. Several examples of Vivaldi antennas with stable phase centers in the frequency band of 2-18 GHz are provided in [15], [16], and [17].

The associate editor coordinating the review of this manuscript and approving it for publication was Davide Ramaccia.

These antennas show improved phase center stability compared to horn antennas. However, they have linear polarization and relatively large dimensions, which pose challenges for low-frequency structures. Reference [14] introduces a rod antenna with a wide BW, linear polarization, and stable phase center. However, fabricating such antennas is challenging. Reference [19] reports a 4-arm cavity-backed spiral antenna with circular polarization and a very stable phase center in the frequency range of 1.1 GHz to 1.7 GHz. Reference [20] presents a triple-band helix antenna that operates in the L, S, and UHF bands with circular polarization and a stable phase center.

After conducting a literature review, we were unable to find an antenna that meets all of the following requirements simultaneously: 1) possessing a super-octave BW, 2) maintaining a stable phase center, 3) exhibiting circular polarization, and 4) featuring compact dimensions and low weight. The development of such an antenna, particularly in the form of an array, is of great importance in DF systems that rely on phase comparison, which is the main focus of our current work. In this article, we present a compact and ultrawideband spiral antenna that encompasses circular polarization and maintains a significantly stable phase center within the frequency range of 2-18 GHz.

II. ANTENNA DESIGN AND CHARACTERISTICS

The primary goal of this study is to develop an antenna that can be used for DF systems. The antenna should have a BW ranging from 2 to 12 GHz, circular polarization, a radiation pattern without any nulls in the broadside direction, and a phase center offset of less than 10 mm. Our proposed antenna design is presented in FIGURE 1. It consists of a dual-arm flat spiral antenna that is printed on a RO4003C dielectric substrate with a thickness of 1.5 mm (the other side of the substrate does not have any copper).

Several equations have been proposed in the past for designing the arms of spiral antennas. After simulating different spirals (Archimedean, logarithmic, and complementary logarithmic), we determined that using the logarithmic spiral antenna results in better impedance matching, circular polarization, wider bandwidth, and improved phase center stability. The equations governing the arm curves of these types of spirals are:

$$x(t) = \frac{D_I}{2}\cos(t)\ \exp\left\{\frac{t}{2N\pi}Ln\left(D_O/D_I\right)\right\}$$
$$y(t) = \frac{D_I}{2}\sin(t)\ \exp\left\{\frac{t}{2N\pi}Ln\left(D_O/D_I\right)\right\} \quad (1)$$

where $0 \leq t \leq 2N\pi$, x and y represent the coordinates of the arms on the antenna plane (xoy), N is the number of turns of the arms, and D_I and D_O are the inner and outer diameters the arms, as depicted in FIGURE 1(a). As shown in FIGURE 1(b), the proposed spiral antenna is backed by an aluminum enclosure (cavity) with a diameter of D_C and a height of H_C. This cavity serves to eliminate back lobes and reflect the signal towards the upper surface of the antenna.

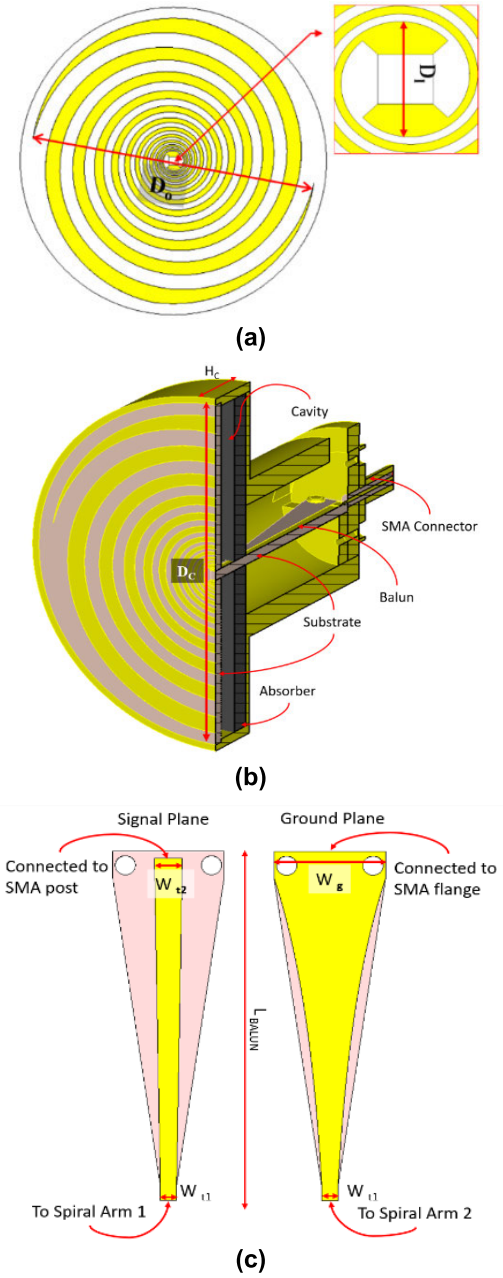

FIGURE 1. Schematic of the proposed spiral antenna: (a) top view, (b) cross section view, and (c) top and bottom view of the microstrip balun.

TABLE 1. Optimized values of the design parameters.

Parameter	Value
N	5.6 Turns
L_{BALUN}	26 mm
D_O	52 mm
D_I	3.5 mm
D_C	58 mm
H_C	9.25 mm
W_g	11 mm
W_{t1}	1.6 mm
W_{t2}	2.7 mm

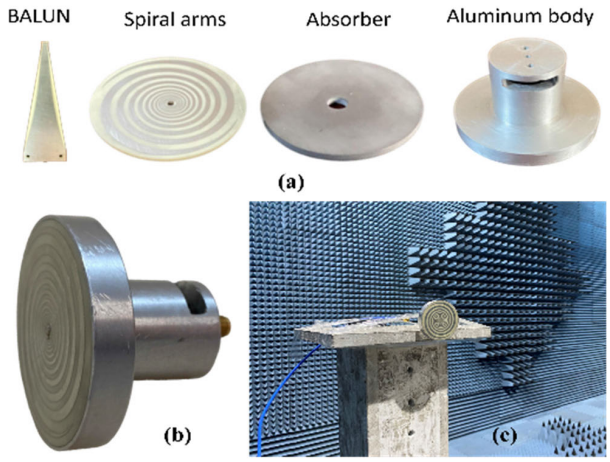

FIGURE 2. Fabricated antenna: (a) dissembled components, (b) antenna after assembly, and (c), antenna in an anechoic chamber.

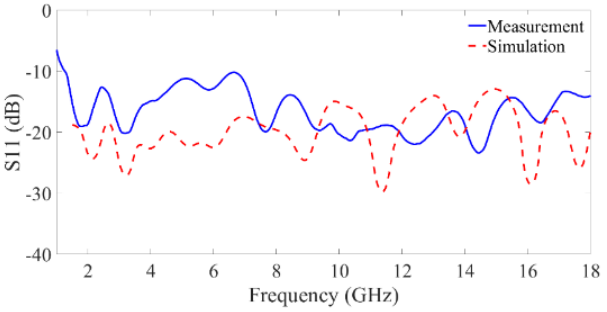

FIGURE 3. Simulated and measured S_{11}.

The height of the cavity is a crucial design parameter, ideally being approximately one-fourth of the wavelength of the center frequency. However, the use of a cavity does have some drawbacks, including a reduction in BW, distortion of the antenna pattern, and significant changes in the phase center or the antenna. To mitigate these negative effects, an absorber is placed on the lower surface of the cavity to eliminate returning signals. The use of an absorber helps reduce interference between disruptive signals, makes the radiation pattern of the antenna symmetric, and enhances both BW and phase center stability. However, it does result in a reduction in antenna gain. Nonetheless, in our target application, which is phase comparison-based DF, the priority is placed on phase center stability rather than gain. This is because phase comparison-based DF algorithms rely on the phase of the signals received by the antenna elements relative to their phase centers, rather than their amplitude [23]. The absorber used in our design is the MF-117 from Laird, which has a standard thickness of 3.2 mm.

For feeding the spiral arms, a microstrip balun is used. The balun is designed on a RO4003C substrate with a thickness of 1.5 mm. The top and bottom surfaces of the balun are shown in FIGURE 1(c). On the signal plane, a coaxial connector post is mounted to a tapered strip with a width of W_{t1}. To match the spiral antenna impedance (approximately 180 Ω) to the 50 Ω reference impedance, the strip is tapered to a width of W_{t2} on the spiral arm side. On the bottom layer of the balun, the width of the ground plane is tapered through an exponential curve from the edge connected to the flange of the connector (W_g) to the edge connected to the spiral arm (W_{t1}).

The design parameters were initially determined using analytical relations and the Antenna Magus software. Subsequently, full-wave electromagnetic simulations were conducted using the CST Studio package. This package allowed us to obtain the phase center offset (PCO) and phase center variation (PCV) of the simulated antenna. To meet the desired specifications, which include a stable phase center in three directions, circular polarization, and proper radiation patterns, optimization and parameter sweeps were performed on the design parameters. The goal was to achieve these specifications over the widest possible BW covering 2 to 12 GHz. The optimized values of the design parameters are given in TABLE 1. Additionally, a more detailed parameter study of the antenna is provided in the Appendix.

During the simulation, we observed the effect of different parameters on the stability of the phase center. Since most of the energy is concentrated in the half-power beamwidth (HPBW) of the antenna, the radiation characteristics in that direction have a significant impact on the phase center. Increasing the height of the cavity or the number of turns of the arms can improve the antenna gain, but it also causes variation in the phase center along the radiation direction.

Furthermore, any disturbance to the physical and radiation symmetry of the antenna in any direction will result in more pronounced changes in the phase center in that particular direction. Therefore, it is important to use symmetric structures as much as possible.

III. RESULTS AND VALIDATION

Following the finalization of the design, the antenna fabrication process was carried out. The spiral arms and balun were fabricated using PCB technology. A square hole with a side length of 1.6 mm was created in the center of the antenna substrate to allow the balun to pass through and connect to the arms. The aluminum body of the antenna was constructed using a CNC machine. As shown in FIGURE 1(b), this unified body consists of a cavity and a balun holder. On one side of the holder, a hole was created to facilitate the mounting of the connector on the balun and screwing the balun onto the holder. The absorber was cut to a suitable size and a hole was made in its center for the balun to pass through. The absorber was then connected to the aluminum body using glue. Finally, the arms of the antenna were soldered to the copper strips of the balun, and an SMA connector was mounted. FIGURE 2(a) shows the disassembled components of the antenna, and FIGURE 2(b) illustrates the antenna after assembly.

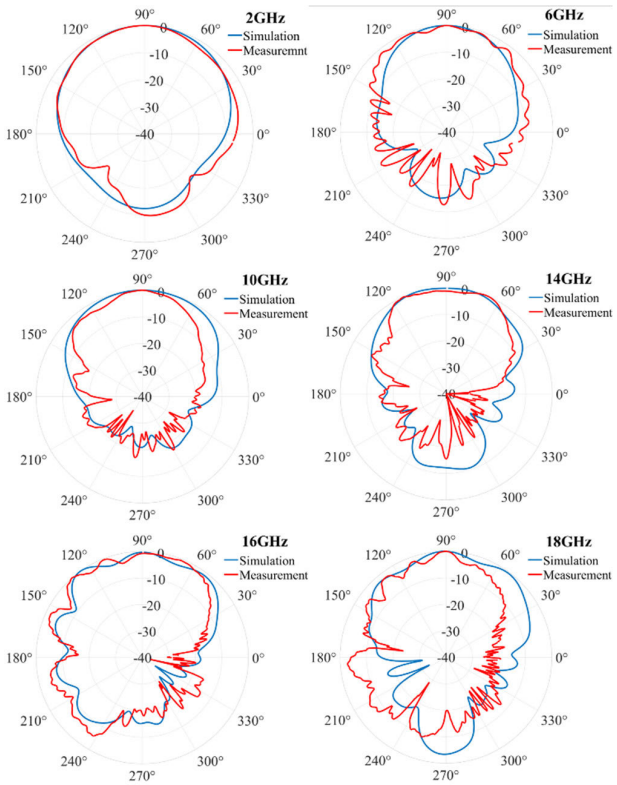

FIGURE 4. Simulated and measured radiation patterns of the absolute field at different frequencies.

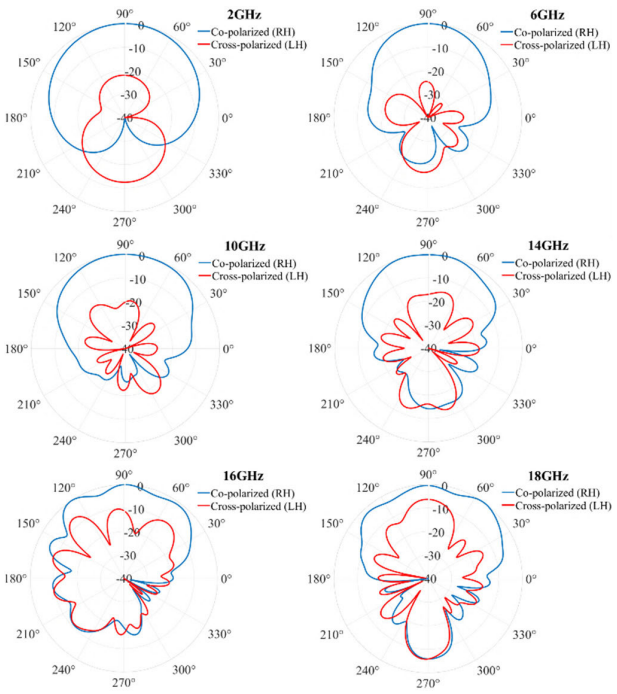

FIGURE 5. Simulated co-polarization (right-handed) and cross-polarization (left-handed) at different frequencies.

The S_{11} of the antenna was measured using a VNA in the frequency range of 1-18 GHz, and the results are presented in FIGURE 3. As observed, both the measurement results and

TABLE 2. Measured values of HPBW and F/B.

F [GHz]	HPBW (deg)	F/B [dB]
2	98	12.6
6	63	16.1
10	80	21.4
14	96	13.3
16	95	15.2
18	72	4.5

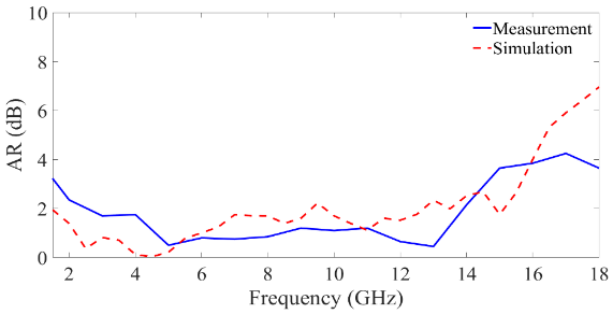

FIGURE 6. Simulated and measured AR.

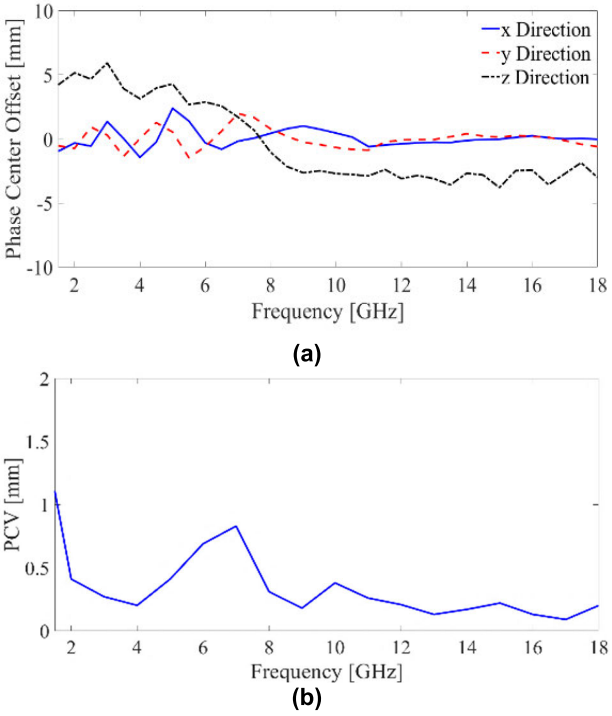

FIGURE 7. Simulated (a) PCO and (b) PCV versus frequency.

simulation indicate an S_{11} below -10 dB in the frequency range of 1.25 GHz to the end of the band, confirming proper wideband matching of the antenna in an ultrawideband. The slight discrepancies between simulation and measurement results for S_{11} are primarily due to mechanical assembly and fabrication inaccuracies, as well as the differences between

TABLE 3. Comparison between the proposed antenna and stable phase center antennas reported in the literature.

Ref.	Antenna Type	Size [mm^3]	10dB RL BW [GHz]	PCV[1] [mm]	PCO[2] [mm]	Polar	3dB AR BW [GHz]	Gain [dBi]	Fab. Cost
[17]	Vivaldi	140×100×0.8	2.0~18.0	N. A.	25	Lin.	-	3~12	Medium
[24]	Vivaldi	100×60×0.8	6.0~18.0	N. A	12	Lin.	-	9.5~15	Medium
[25]	Vivaldi	100×60×0.8	3.0~22.0	N. A.	15	Lin.	-	10~15	Low
[26]	Slot	80×80×5	1.4~1.7	N. A.	1	Cir.	1.58	-1~4.5	Low
[3]	Crossed Slot	125×125×35	1.1~1.7	4.5	N.A.	Cir.	1.1~1.65	2~6.3	Low
[4]	Horn	80×80×160	6.0~20.0	40	45	Lin.	-	12.5~17.5	Medium
[27]	Crossed Dipole	80×80×27	1.0~2.0	3	1.1	Cir.	1.1~1.9	0~5	Medium
[28]	Inverted F	300×100×25	1.4~1.8	3.5	N.A.	Cir.	1.2~1.9	1~7.5	Low
[29]	Conical Log-Spiral	210×210×170	2.0~14.0	N.A.	45	Cir.	2~14	N.A.	High
This Work	**Spiral**	**58×58×50**	**1.25~18**	**1.1**	**10**	**Cir.**	**1.5~16**	**-1~3.5**	**Medium**

[1] *Maximum simulated PCV across the operating BW.*
[2] *Maximum change in the simulated PCO across the operating BW.*

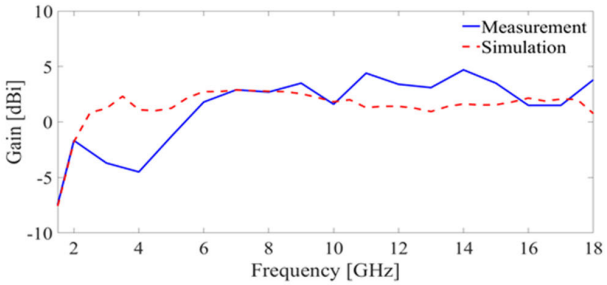

FIGURE 8. Simulated and measured realized gain.

the idealized simulation environment and the actual measurement conditions.

The radiation characteristics of the antenna were tested in an anechoic chamber room in the frequency range of 1.25 to 18 GHz (where S_{11} is below -10 dB), as shown in FIGURE 2(c). FIGURE 4 presents the absolute radiation patterns of the antenna at frequencies 2, 6, 10, 14, 16, and 18 GHz. The patterns on the broad side do not contain any nulls. The measured values of the HPBW and front-to-back ratio (F/B) at the measured frequencies are listed in TABLE 2. It is evident that the HPBW exceeds 60 degrees across the entire bandwidth. It is important to note that a HPBW greater than 60 degrees is desirable in DF applications. In addition, FIGURE 5 shows the simulated right- and left-handed circular polarization (RCP and LCP) patterns, representing the co- and cross-polarization patterns of the antenna, respectively. The cross-polarized pattern is observed to be 10 dB lower than the co-polarized pattern up to 16 GHz. This suggests that a good axial ratio (AR) can be expected up to this frequency.

FIGURE 6 presents the measured and simulated AR of the antenna. Within the 2-16 GHz frequency band, both the simulated and measured results indicate AR values below 3 dB. Furthermore, from 1.25 GHz to 18 GHz, the AR remains below 4 dB, confirming the achievement of circular polarization across this band.

In FIGURE 7(a), we present the variation of the PCO in the x, y, and z directions. As shown in the figure, the PCO changes are less than 4 mm along the x and y directions, and less than 10 mm along the z direction across the entire BW (1.25-18 GHz). The PCV is also shown in FIGURE 7(b), demonstrating a low PCV of less than around 1 mm which is equivalent to a high accuracy of the phase center. It is important to note that due to the infeasibility of measuring the phase center in the antenna chamber, we relied solely on simulation results.

Additionally, FIGURE 8 depicts the simulated and measured realized gain of the antenna, showing good agreement. The antenna gain varies between -4.5 dB (-7 dB) to 4.7 dB in the frequency range of 2 GHz (1.25 GHz) to 18 GHz. It is worth noting that the lower gain at lower frequencies is due to the small dimensions of the antenna. The use of the absorber in the antenna has also led to a reduction in gain. However, as previously discussed, in the target application of this work (DF based on phase comparison), the antenna gain is not significantly important. It is also worth noting that the discrepancy between simulated and measured gain values can be attributed to inaccuracies in the measurement setup. As seen in FIGURE 2(c), the antenna was installed on a significantly large MDF fixture, which could have caused scattered fields from the fixture, thereby leading to measurement errors.

By analyzing the results presented above, it can be concluded that the objectives of this work have been

successfully met. Not only were they achieved within the desired frequency range of 2-12 GHz, but they were also accomplished in a wider BW of 1.25-18 GHz.

Finally, TABLE 3 presents a comparison between our work and previous studies that have reported on the stability of the phase center in a wideband. This comparison highlights the unique features of our antenna, including its compact size, circular polarization, and excellent phase center stability (PCO $<$ 10 mm) and accuracy (PCV $<$ 1.1 mm) across the 1.25-18 GHz BW. Notably, none of the antennas listed in the table below exhibit this combination of features.

IV. CONCLUSION

In this article, we presented the design and fabrication of an ultrawideband antenna with circular polarization and a highly stable phase center for DF applications. The antenna is a cavity backed log-spiral arms with an absorber placed behind it to ensure phase center stability. Simulation results and measurements demonstrate that the antenna exhibits impedance matching from 1.25 to 18 GHz. Within this frequency band, the antenna has also a phase center offset of less than 10 mm in the direction of radiation and less than 4 mm in the plane of the spiral arms. The PCV is also found to be less than 1.11 mm. Furthermore, within the frequency band of 1.25 GHz to 16 GHz (18 GHz), the antenna achieves an AR of less than 3 dB (4 dB). Finally, the measured gain ranges from −4.5 dB to 4.7 dB in a 2-18 GHz BW.

APPENDIX

In this appendix, we present additional details and studies to demonstrate the effect of different design parameters on the antenna's performance. FIGURE 9 shows the performance of the antenna with and without the absorber material. It can be observed that adding the absorber to the bottom of the cavity

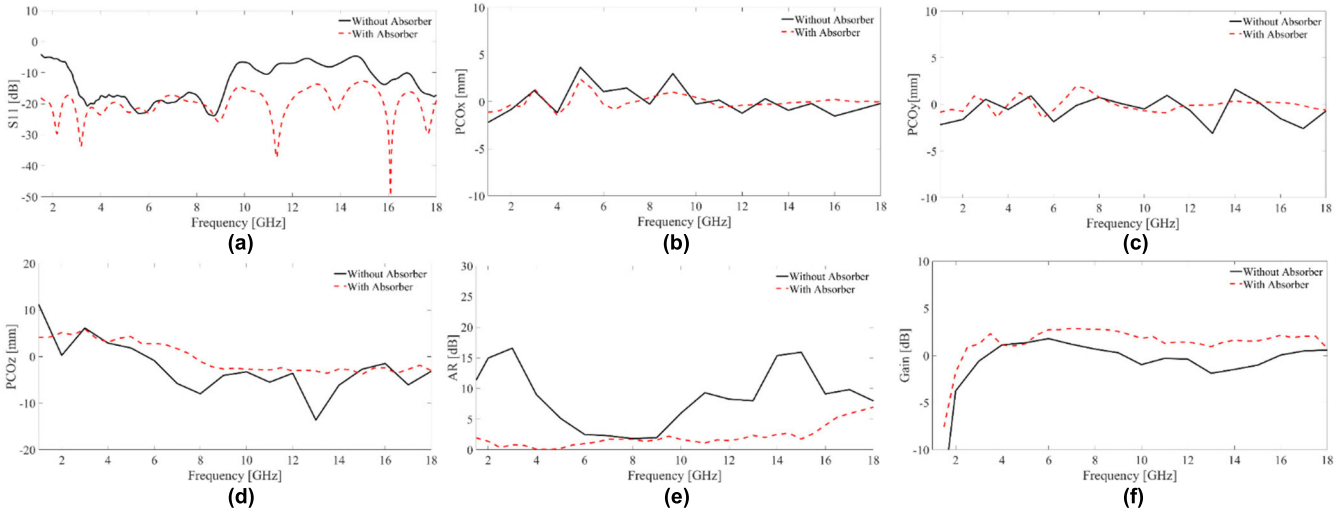

FIGURE 9. Antenna performance with and without employing the absorber on the bottom of the cavity: S_{11} (a), PCO variations in x (b), y (c), and z (d) directions, AR (e), and gain (f).

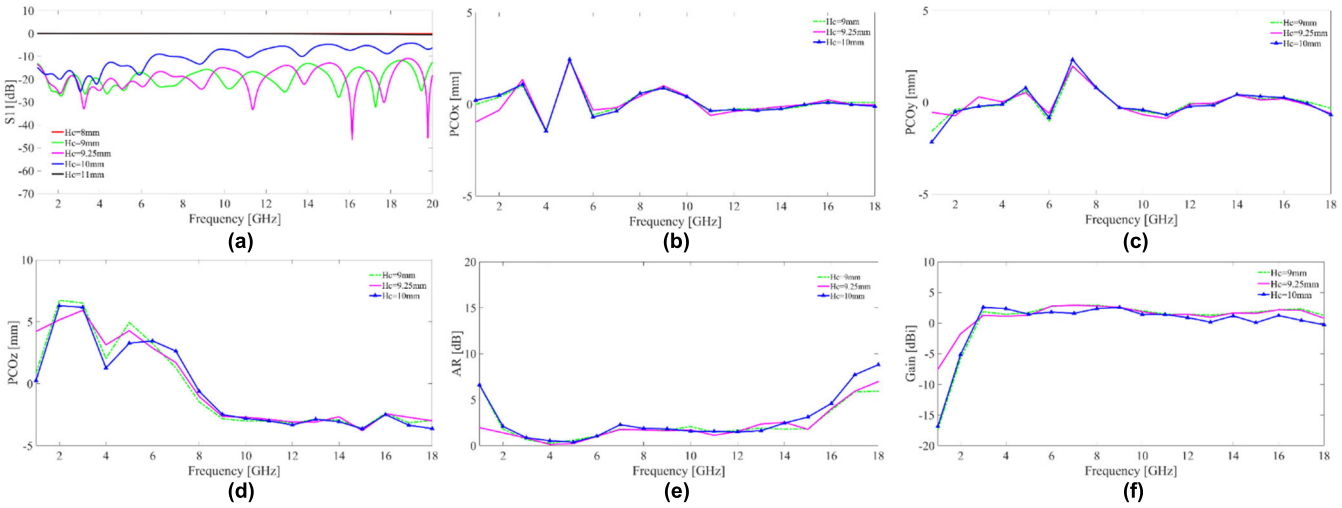

FIGURE 10. Antenna performance for different values of the cavity height (the values of other design parameter were kept fixed as given in TABLE 1): S_{11} (a), PCO variations in x (b), y (c), and z (d) directions, AR (e), and gain (f).

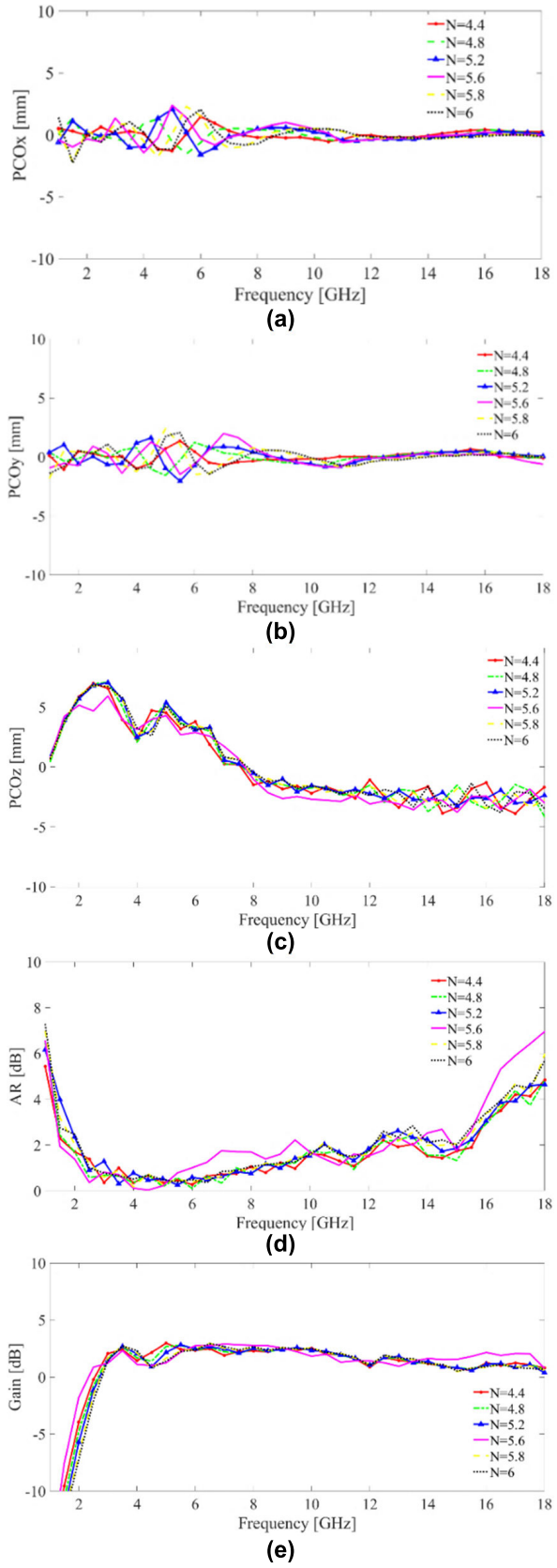

FIGURE 11. Antenna performance for different number of turns of the antenna arms (the values of other design parameter were kept fixed as given in TABLE 1): PCO variations in x (a), y (b), and z (c) directions, AR (d), and gain (e).

not only expands the bandwidth but also stabilizes the PCO, though it slightly reduces the gain.

We also examine the impact of two parameters: the height of the cavity (H_C) and the number of turns of the antenna arms (N). The results of these studies are shown in FIGURES 10 and 11, respectively. FIGURE 10(a) illustrates that HC significantly affects the impedance matching of the antenna. For optimal matching within the frequency band of interest, HC should be around 9 mm. FIGURES 10(b)-(d) show that the PCO variation is consistent for H_C values of 9, 9.25, and 10 mm. However, FIGURES 10(e) and (f) demonstrate that the AR and gain are more desirable when H_C is set to 9.25 mm. Furthermore, FIGURE 11(c) indicates that the optimal value of N, which is 5.6, provides better PCO variation in the z-direction, while other parameters (PCO variation in other directions, AR, and gain) do not show significant changes for different values of N between 4 to 6.

REFERENCES

[1] C. A. Balanis, *Antenna Theory: Analysis and Design*, 4th ed., Hoboken, NJ, USA: Wiley, 2016.

[2] G. A. Bartels, *GPS-Antenna Phase Center Measurements Performed in an Anechoic Chamber*. Delft, The Netherlands: Delft Univ. Press, 1997.

[3] H. Zhang, Y. Guo, and G. Wang, "A wideband circularly polarized crossed-slot antenna with stable phase center," *IEEE Antennas Wireless Propag. Lett.*, vol. 18, pp. 941–945, 2019.

[4] S. Manshari, S. Koziel, and L. Leifsson, "A wideband corrugated ridged horn antenna with enhanced gain and stable phase center for X- and Ku-band applications," *IEEE Antennas Wireless Propag. Lett.*, vol. 18, pp. 1031–1035, 2019.

[5] O. Montenbruck, M. Garcia-Fernandez, Y. Yoon, S. Schön, and A. Jäggi, "Antenna phase center calibration for precise positioning of LEO satellites," *GPS Solutions*, vol. 13, no. 1, pp. 23–34, Jan. 2009.

[6] N. T. Tokan, "Optimization of the UWB feed antenna position in reflector applications," *Int. J. Antennas Propag.*, vol. 2014, pp. 1–7, Aug. 2014.

[7] Z. Li, J. Chen, L. Zhen, S. Cui, K. G. Shin, and J. Liu, "Coordinated multipoint transmissions based on interference alignment and neutralization," *IEEE Trans. Wireless Commun.*, vol. 18, no. 7, pp. 3347–3365, Jul. 2019.

[8] P. Willis, B. J. Haines, and D. Kuang, "DORIS satellite phase center determination and consequences on the derived scale of the terrestrial reference frame," *Adv. Space Res.*, vol. 39, no. 10, pp. 1589–1596, Jan. 2007.

[9] R. Zhou, Z. Hu, Q. Zhao, H. Cai, X. Liu, C. Liu, G. Wang, H. Kan, and L. Chen, "Consistency analysis of the GNSS antenna phase center correction models," *Remote Sens.*, vol. 14, no. 3, p. 540, Jan. 2022.

[10] C. Ehrenborg, "Investigation and comparison between radiation and phase center for canonical antennas," M.S. thesis, Dept. Elect. Inf. Technol., Lund Univ., Sweden, Europe, 2014.

[11] B. H. Simakauskas, "Phase center stabilization of a horn antenna and its application in a Luneburg lens feed array," M.S. thesis, Dept. Elect. Comput. Energy Eng., Univ. Colorado, Boulder, CO, USA, 2015.

[12] A. K. Baghel, S. S. Kulkarni, and S. K. Nayak, "A high gain aperture match parabolic horn antenna with stable phase center and higher FBR in S-band," *Microwave Opt. Technol. Lett.*, vol. 63, no. 8, pp. 2179–2185, Aug. 2021.

[13] A. A. Generalov, J. A. Haimakainen, D. V. Lioubtchenko, and A. V. Räisänen, "Wide band mm- and sub-mm-Wave dielectric rod waveguide antenna," *IEEE Trans. Terahertz Sci. Technol.*, vol. 4, no. 5, pp. 568–574, Sep. 2014.

[14] C.-W. Liu and C.-C. Chen, "A UWB three-layer dielectric rod antenna with constant gain, pattern and phase center," *IEEE Trans. Antennas Propag.*, vol. 60, no. 10, pp. 4500–4508, Oct. 2012.

[15] Y. W. Wang, G. M. Wang, Z. W. Yu, J. G. Liang, and X. J. Gao, "UltraWideband E-plane monopulse antenna using Vivaldi antenna," *IEEE Trans. Antennas Propag.*, vol. 62, no. 10, pp. 4961–4969, Oct. 2014.

[16] S. Zhang, "Modified Vivaldi antenna with improved gain and phase center stability," in *Proc. Prog. Electromagn. Res. Symp. (PIERS)*, 2016, pp. 108–111.

[17] A. Saee Arezoomand, R. A. Sadeghzadeh, and M. Naser-Moghadasi, "Investigation and improvement of the phase-center characteristics of Vivaldi's antenna for UWB applications," *Microwave Opt. Technol. Lett.*, vol. 58, no. 6, pp. 1275–1281, Mar. 2016.
[18] Y. Pan and Y. Dong, "Low-profile low-cost ultra-wideband circularly polarized slot antennas," *IEEE Access*, vol. 7, pp. 160696–160704, 2019.
[19] L. Guo, P. Zhang, F. Zeng, Z. Zhang, and C. Zhang, "A novel four-arm planar spiral antenna for GNSS application," *IEEE Access*, vol. 9, pp. 168899–168906, 2021.
[20] X. Bai, J. Tang, X. Liang, J. Geng, and R. Jin, "Compact design of triple-band circularly polarized quadrifilar helix antennas," *IEEE Antennas Wireless Propag. Lett.*, vol. 13, pp. 380–383, 2014.
[21] Y.-W. Zhong, G.-M. Yang, J.-Y. Mo, and L.-R. Zheng, "Compact circularly polarized Archimedean spiral antenna for ultrawideband communication applications," *IEEE Antennas Wireless Propag. Lett.*, vol. 16, pp. 129–132, 2017.
[22] S. Wang, H. Li, Y. Zhang, J. Long, and E. Li, "A helix-loaded equiangular spiral antenna with compact structure," in *Proc. 12th Int. Symp. Antennas, Propag. EM Theory (ISAPE)*, Dec. 2018, pp. 1–4.
[23] R. Ardoino. *Passive Direction Finding (DF) Techniques—Phase Comparison*. Accessed: Aug. 3, 2024. [Online]. Available: https://www.emsopedia.org/entries/passive-direction-finding-df
[24] A. S. Arezoomand, M. Naser-Moghadasi, I. Arghand, P. Jahangiri, and F. B. Zarrabi, "Photonic band gap implementation for phase centre controlling in Vivaldi antenna," *IET Microwave, Antennas Propag.*, vol. 11, no. 13, pp. 1880–1886, Oct. 2017.
[25] A. S. Arezoomand, R.-A. Sadeghzadeh, and M. Naser-Moghadasi, "Novel techniques in tapered slot antenna for linearity phase center and gain enhancement," *IEEE Antennas Wireless Propag. Lett.*, vol. 16, pp. 270–273, 2017.
[26] K.-K. Zheng and Q.-X. Chu, "A novel annular slotted center-fed BeiDou antenna with a stable phase center," *IEEE Antennas Wireless Propag. Lett.*, vol. 17, pp. 364–367, 2018.
[27] H. Zhang, Y. Guo, and G. Wang, "A design of wideband circularly polarized antenna with stable phase center over the whole GNSS bands," *IEEE Antennas Wireless Propag. Lett.*, vol. 18, pp. 2746–2750, 2019.
[28] H. Zhang, G. Tang, X. Du, J. Ren, and Y. Z. Yin, "Design of a multi-fed combined circularly polarized inverted-F antenna with stable phase center," *Int. J. RF Microwave Comput.-Aided Eng.*, vol. 31, no. 11, Nov. 2021, Art. no. e22861.
[29] K. A. Abdalmalak, G. Santamaría Botello, S. Llorente-Romano, A. Rivera-Lavado, J. Flygare, J. A. López Fernándezs, J. M. Serna Puente, L. E. García-Castillo, D. Segovia-Vargas, M. Pantaleev, and L. E. García-Muñoz, "Ultrawideband conical log-spiral circularly polarized feed for radio astronomy," *IEEE Trans. Antennas Propag.*, vol. 68, no. 3, pp. 1995–2007, Mar. 2020.

AMIRHOSSEIN MOUSAVIKHAH was born in Sabzevar, Iran. He received the B.Sc. degree in electrical engineering from Shahrood University of Technology (SUT), Shahrud, Iran, in 2020, and the M.Sc. degree in space engineering from Iran University of Science and Technology (IUST), Tehran, Iran, in 2023.

His research interests include microwave filters, metamaterials, and antennas.

VAHID NAYYERI (Senior Member, IEEE) was born in Tehran, Iran, in 1983. He received the B.Sc. degree in electrical engineering from Iran University of Science and Technology (IUST), Tehran, in 2006, the M.Sc. degree in electrical engineering from the University of Tehran, Tehran, in 2008, and the Ph.D. degree in electrical engineering from IUST, in 2013.

From 2007 to 2013, he was a Research Assistant with IUST and then a Visiting Scholar with the University of Waterloo, ON, Canada. In 2013, he joined the Faculty of IUST, where he is currently an Associate Professor, the Director of the "Advanced Radio Circuits and Systems Laboratory," and the Head of the Department of Satellite Technology. In 2019, he was a Visiting Professor with the University of Waterloo. He has authored and co-authored one book (in Persian), one book chapter, and more than 120 technical articles. His research interests include microwave active and passive circuits and applied and computational electromagnetics.

Dr. Nayyeri serves the IEEE Iran Section as a Member of the Board of Directors and a Steering Committee Member for the Electromagnetics and Photonics Chapter. He received the Best Ph.D. Thesis Award from the IEEE Iran Section, in 2014. He was also awarded the 2024 Raj Mittra Travel Grant (RMTG) from IEEE AP/S. In 2019 and 2020, he served as a Guest Editor for two special issues of *Sensors*. He is an Associate Editor of IEEE TRANSACTIONS ON MICROWAVES THEORY TECHNIQUES and *IET Microwaves, Antennas and Propagation*. He is the Chair of the Membership Development Committee.

MOSTAFA KHANJARIAN was born in Aleshtar, Iran, in 1992. He received the B.Sc. degree in electrical engineering from Isfahan University of Technology (IUT), Isfahan, Iran, in 2014, and the M.Sc. degree in electrical engineering from Iran University of Science and Technology (IUST), Tehran, Iran, in 2016, where he is currently pursuing the Ph.D. degree in electrical engineering.

His research interests include antennas, metasurfaces, and microwave circuits.